Predicting Individualized Joint Kinematics over a Continuous Range of Slopes and Speeds

Emma Reznick[1], Kyle Embry[2], and Robert D. Gregg[3], *Senior Member, IEEE*

***Abstract*— Individuality in clinical gait analysis is often quantified by an individual's kinematic deviation from the norm, but it is unclear how these deviations generalize across different walking speeds and ground slopes. Understanding individuality across tasks has important implications in the tuning of prosthetic legs, where clinicians have limited time and resources to personalize the kinematic motion of the leg to therapeutically enhance the wearer's gait. This study seeks to determine an efficient way to predictively model an individual's kinematics over a continuous range of slopes and speeds given only one personalized task at level ground. We were able to predict the kinematics of able-bodied individuals at a wide variety of conditions that were not specifically tuned. Applied to 10 human subjects, the individualization method reduced the RMSE between the model and subject's kinematics over all tasks by an average of 2% (max 52%) at the ankle, 27% (max 59%) at the knee, and 45% (max 83%) at the hip. Our results indicate that knowing how an individual subject differs from the average subject at level ground alone is enough information to improve kinematic predictions across all tasks. This research offers a new method for personalizing robotic prosthetic legs over a variety of tasks without the need of an engineer, which could make these complex devices more clinically viable.**

I. Introduction

Tuning a prosthetic device to an individual can therapeutically enhance their gait [1], [2]. Currently, powered robotic prostheses that adapt to multiple conditions take prohibitively long to individualize [3] and usually require the assistance of an engineer [1], [3], resulting in a barrier to clinical viability. These complex devices have the potential to increase the speed and efficacy of gait rehabilitation [4], but tuning the software of robotic prostheses often falls beyond the scope of a clinician's knowledge. Prostheses must be individualized, or tuned, appropriately for an individual's gait to increase symmetry, improve leg function, and minimize gait compensations that lead to overuse injuries [5]. Due to differences in how individuals walk, tuning is crucial for the successful use of prostheses [6] like microprocessor knees and actuated robotic knee-ankle prosthetic legs [7], [8]. The overarching goal of tuning a prosthesis is to restore normative gait to an amputee in a manner that suits the individual. The presented individualization process shows that tuning multiple tasks can be intuitive and clinically viable.

Simplifying the tuning process of robotic prostheses will make them more accessible to clinicians who understand the intricate process of gait rehabilitation, but lack the specific knowledge of an engineer or manufacturer representative [1], [2]. Quintero et al. bridged the knowledge gap between engineers and clinicians by using an intuitive interface to manipulate the flexion and extension of a knee and ankle prosthesis throughout the gait cycle, i.e., the joint angle trajectories. In their case study, the clinician was able to efficiently tune a complex prosthesis for a single level-ground walking task using this method [1].

Individual gait patterns are unique [9], [10] and used in many applications from individualized medical diagnostics [10] to prosthetic motion [11]. Recently, researchers have determined how factors such as gender, age, walking speed, and BMI contribute to an individual's gait [12], [13]. Terrain grade, or slope, is often overlooked in gait individuality studies, but is a significant parameter affecting joint kinematics [14], [15]. Embry et al. created a predictive model that represents gait kinematics as a continuous function of gait phase, speed, and slope. This model was trained from population mean joint trajectories at samples of slope and speed–the 'task'–and can accurately predict mean joint trajectories over a continuous range of these tasks [15]. This can be used to drive a prosthetic controller that can easily be tuned (as suggested in [16]), but as it fits the average user, the model does not account for individuality. It may be possible to leverage the continuous-task kinematic model from [15] and the kinematic tuning method from [1] to establish a new method for individualizing joint kinematics of a prosthesis over a continuous range of tasks. Specifically, we hypothesize that because the kinematic model from [15] continuously links all tasks, it can be used to distribute individual features from a single tuned task across the entire model.

In this study, we develop the theoretical framework for tuning a prosthesis for tasks that are often difficult to replicate in a clinic, such as multiple slopes. This specific application aims to model individual kinematics across tasks based only on personalized data for level-ground walking at a normal speed. When used to change the motion of a powered prosthetic leg, this individualized model would reduce the time it takes to tune multiple tasks and shift the onus of tuning from engineers to clinicians. The presented data-driven study lays the groundwork for clinical individualization of a powered prosthetic leg over continuously varying tasks. In Section II, we will discuss the methods used for

[1] E. Reznick is with the Department of Bioengineering and [2] K. Embry is with the Department of Mechanical Engineering at the University of Texas at Dallas, Richardson, TX 75080, USA. [3] R. Gregg is with the Department of Electrical Engineering and Computer Science and the Robotics Institute at the University of Michigan, Ann Arbor, MI 48109, USA. Email: [1]emma.reznick@utdallas.edu; [3]rdgregg@umich.edu.

This work was supported by the National Institute of Child Health & Human Development of the NIH under Award Number R01HD09477. The content is solely the responsibility of the authors and does not necessarily represent the official views of the NIH. R. D. Gregg holds a Career Award at the Scientific Interface from the Burroughs Wellcome Fund.

obtaining the able-bodied data set, modeling kinematics of a continuous range of tasks, quantifying individuality by defining the individual's specific contribution, and individualizing the model. In Section III, we will discuss the accuracy of trajectory design and how well the individualized trajectories and models express an individual's unique gait across all tasks. Finally, in Section IV, we discuss the implications of this modeling scheme for a representative subject.

II. Methods

A. Data Set

The data used for this study was collected for a related study [15] and is accessible for download from IEEE Dataport [17]. The experimental protocol and subsequent analysis was approved by the Institutional Review Board at the University of Texas at Dallas and the University of Michigan. All 10 subjects (5 female) were able-bodied and provided written informed consent. The subjects had a mean age of 23 years (SD = 2.8 years), mean height of 170 cm (SD = 8.2 cm), and mean weight of 64 kg (SD = 7.7 kg). A 10-camera Vicon T40 motion capture system (Vicon, Oxford, UK) recorded the subjects' kinematics at 100 Hz. All tests consisted of subjects walking at a steady speed and grade on a Bertec instrumented split-belt treadmill (Bertec Corp., Columbus, OH) for one minute. For each test, data was collected while the subject walked at a constant speed of 0.8, 1.0, or 1.2 m/s and a constant ground slope ranging from -10° to +10° at 2.5° increments. All subjects walked at every combination of speed and slope, resulting in 27 different tasks with unique identifiers, χ_j with $j = 1, 2, ..., 27$. The order of trials was randomized and subjects took breaks to prevent fatigue [15]. In the dataset, strides were normalized over time and interpolated over 150 points in phase.

B. Format of Basis Model

Embry et al. [15] created a predictive model that represents inter-subject mean gait kinematics as a continuous function of gait phase and task. Gait phase is represented by a phase variable, $\varphi \in \{\mathbb{R} | 0 \leq \varphi < 1, \dot{\varphi} > 0\}$, which is a cyclic and monotonic scalar that increases from 0 to 1 once per stride (e.g., [16]). Task is represented by $\chi = (\nu, \alpha)$, where ν is the subject's speed linearly mapped from a range of 0.6 m/s to 1.4 m/s to a range of 0 to 1, and α is the ground slope, linearly mapped from -10° to 10° to a range of 0 to 1.

Gait kinematics are modeled as the weighted summation of N basis functions of phase, $b_k(\varphi)$. The weight of each basis function changes for each unique task, as determined by the task functions $c_k(\chi)$. This yields the following separable expression for the joint angle q of the hip, knee, or ankle:

$$q(\varphi, \chi) = \sum_{k=1}^{N} b_k(\varphi) c_k(\chi), \tag{1}$$

where the number of basis functions is N, indexed by k.

The basis functions $b_k(\varphi)$ model how joint kinematics change in response to the progression of the gait cycle. Basis functions are parameterized as finite Fourier series of degree $F = 10$ with unknown coefficients, which are solved for later. The scalar task functions $c_k(\chi)$ model how joint kinematics change in response to speed and slope. Task functions are modeled as 2nd or 3rd degree Bernstein basis polynomials for the terms that operate on speed or slope (see [15, (3)] for details). Together, these basis and task functions create a kinematic model $q(\varphi, \chi)$ that parameterizes how phase, speed, and slope affect the joint kinematics.

The format of the basis model is linear with respect to the parameters of the basis functions, meaning that for a given φ_i and χ_j:

$$\Lambda_{ij} x = \sum_{k=1}^{N} b_k(\varphi_i) c_k(\chi_j), \tag{2}$$

where $x \in \mathbb{R}^{N(1+2F)}$ is a concatenation of the Fourier coefficients from b_k for $k = 1, \ldots, N$. All other terms, which are constants for a given value of φ_i and χ_j, are collected in vector $\Lambda_{ij} \in \mathbb{R}^{1 \times N(1+2F)}$. See [15, (5)] for details.

C. Basis Model Optimization

The data includes hip, knee, and ankle angular positions at a variety of phases and tasks as described in Section II-A. We can solve for x such that (1) optimally fits this data. Optimality is defined by this objective function and constraints:

$$\begin{aligned}
\underset{x}{\text{minimize}} \quad & \rho + \delta ||\text{vec}(\frac{\partial^3}{\partial \varphi^3} \Lambda_{ij} x)||_2, \\
\text{such that} \quad & -\rho \text{SE}(\mathbf{d}_{\varphi_i \chi_j}) \leq \bar{\mathbf{d}}_{\varphi_i \chi_j} - \Lambda_{ij} x \leq \rho \text{SE}(\mathbf{d}_{\varphi_i \chi_j}), \\
& R_{\min} < \min_m \Lambda_{im} x, \\
& R_{\max} > \max_m \Lambda_{im} x, \\
& \forall\ i = 1, 2, ..., 150, \forall\ m = 1, 2, \ldots, 100, \\
& \text{and } \forall j = 1, 2, \ldots, 27,
\end{aligned} \tag{3}$$

where $\bar{\mathbf{d}}_{\varphi_i \chi_j}$ represents the inter-subject mean joint angular position of the hip, knee, or ankle recorded at a discrete phase φ_i and task χ_j, and $\text{SE}(\mathbf{d}_{\varphi_i \chi_j})$ represents the standard error of all of the subjects at the given task. This optimization problem seeks to minimize two objectives, ρ and $||\text{vec}(\frac{\partial^3}{\partial \varphi^3} \Lambda_{ij} x)||_2$. Scalar value ρ acts as a bound on the absolute difference between the inter-subject mean $\bar{\mathbf{d}}_{\varphi_i \chi_j}$ and the value of the basis model evaluated at the same point in phase and task, $\Lambda_{ij} x$. The difference in these two tasks is multiplied by the reciprocal of the inter-subject standard error $\text{SE}(\mathbf{d}_{\varphi_i \chi_j})$. The logic behind this term is that, if all of our subjects had very similar kinematics at a given point (small standard error), it is more important for our mean kinematic surface to match closely at these points. The second objective term, $||\text{vec}(\frac{\partial^3}{\partial \varphi^3} \Lambda_{ij} x)||_2$, is a measurement of the jerk in the phase dimension of the basis model. The human body tends to move with jerk-minimized trajectories, and this objective strives to improve biomimicry [18], [19]. Our two objectives, fitting to the available data and reducing jerk, are scalarized with a coefficient δ. Lastly, we also constrain that the model always stays within range of motion bounds $R_{\min}$ and $R_{\max}$. We check this bound at 100 evenly spaced values of speed

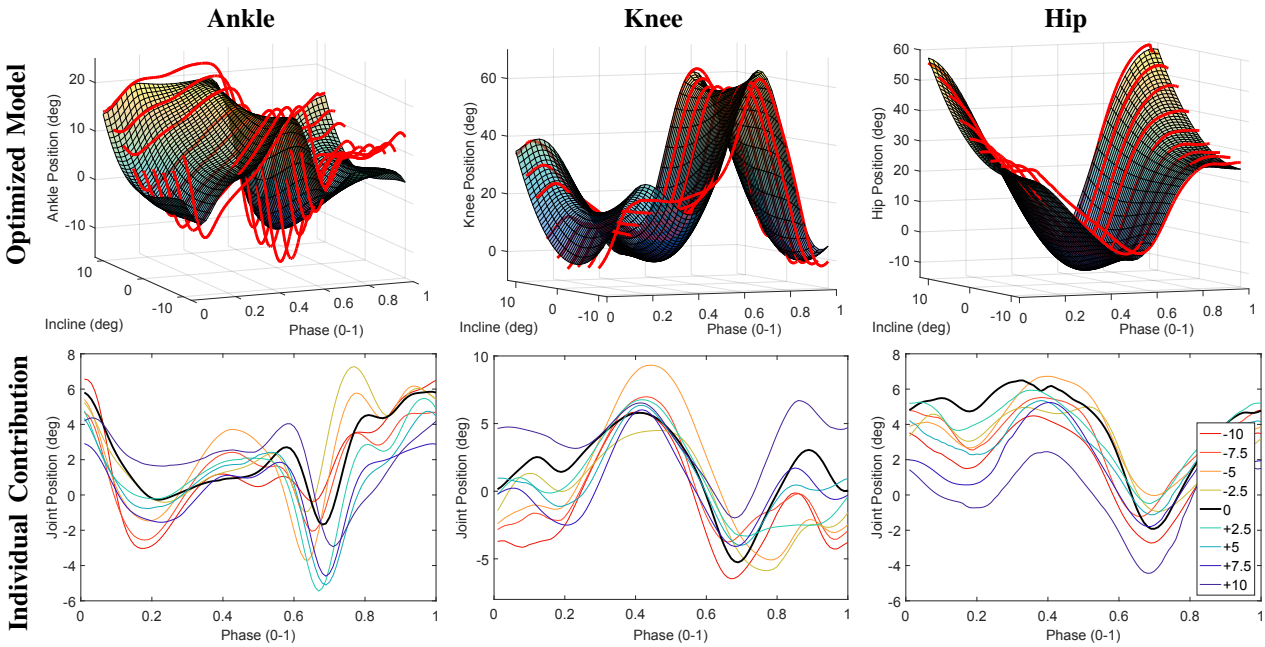

Fig. 1: The top row shows the Basis model surfaces for the ankle, knee, and hip at normal speed, superimposed with one subject's experimental data in red. The bottom row shows the difference between the same subject's experimental data and the inter-subject mean for normal speed at all sampled inclines (in degrees). The difference for the level ground task corresponds to the individual's contribution, shown in bold black.

and grade, indexed by m. This optimization problem can easily be solved with a convex optimization solver like [20], and has a guaranteed globally optimal solution.

D. Modifications to Basis Model

The basis model is trained on mean kinematics across task and phase ($\bar{\mathbf{d}}_{\varphi_i \chi_j}$), while this paper concerns tailoring the model for an individual subject, indexed by η_p with $p = 1, 2, \ldots, 10$. As seen in Fig. 1, the basis model accounts for trends over task, but was not designed to fit an individual's unique kinematics. For this purpose, adjustments must be made to the training trajectories, so that they emulate the individual's unique kinematics, and to the optimization protocol, so that it adapts well to individualized trajectories.

1) Individualization of Training Trajectories: While the basis model can be trained on the complete experimental data of one subject, the objective of this study is to individualize the model under the assumption that only one task is known; specifically the clinically relevant task, self-selected speed over level ground. For the purpose of this study, we assume this task to be normal speed, level ground, χ_B. As the individual's only known task, all individuality in the model stems from the difference between the individual's trajectory $\mathbf{d}_{\varphi_i \chi_B \eta_p}$ and the inter-subject mean $\bar{\mathbf{d}}_{\varphi_i \chi_B}$. We have found that the difference between individual and mean trajectories often follows the same trend across all tasks, seen in Fig. 1 (bottom), and the presented individualization technique is based on this assumption. Therefore, taking the difference at χ_B is a good estimation of the individual's 'contribution' to gait, defined as $C_{\varphi_i \eta_p} = \mathbf{d}_{\varphi_i \chi_B \eta_p} - \bar{\mathbf{d}}_{\varphi_i \chi_B}$. This contribution is added to the inter-subject mean trajectory of each task, $\bar{\mathbf{d}}_{\varphi_i \chi_j} + C_{\varphi_i \eta_p}$, to create a set of individualized trajectories.

2) Modifications to Error Handling: The optimal solution for this modeling problem is found by minimizing the difference, or residual, between the training data and the modeled kinematic surface. This works by employing p-norms (L^p), which are functions that apply penalties to each residual. The type of norm used will encourage different distributions of optimal residuals by applying penalties in a different manner [21]. The basis model used the L^∞ norm in (3), which penalizes the absolute value of the largest residual. As a note, while the L^∞ norm is not written in the problem statement, minimizing ρ, which is constrained to be a bound on the residual between the data and model, acts as an implicit L^∞ norm. This method worked well for inter-subject mean kinematics, but the solutions it found were not well suited for individualized models. To allow for individuality, we categorize the training trajectories into higher and lower priorities so the optimization protocol is more lenient in fitting low-priority tasks. This is accomplished by minimizing the high-priority trajectories using the L^∞ norm, encouraging the model to fit these trajectories closely. The low-priority trajectories are penalized by the L^2 norm, which applies quadratic penalties to residuals, encouraging a normal, unbounded, distribution of optimal residuals [21]. We elected to use $\mathbf{d}_{\varphi_i \chi_B \eta_p}$ and the individualized normal-speed $\pm 10°$ tasks for high-priority fitting so that the model would exactly fit the true individual trajectory at χ_B and carry the individual contribution out to the most extreme modeled tasks. It should be noted that the high-priority $\pm 10°$ tasks are designed using the same individualization method as the low-priority tasks. The low-priority trajectories were

TABLE I: Training trajectory RMSE and max error across all tasks for all subjects and joints. The top half of the table pertains to the inter-subject mean trajectories and the bottom half refers to the individualized trajectories. The last column shows the mean RMSE or max error at each joint across all subjects. Significantly decreased values are marked with a '*' and all values are reported in degrees.

		AB01	AB02	AB03	AB04	AB05	AB06	AB07	AB08	AB09	AB10	Mean	SD
Subject Average RMSE	Ankle	2.74	2.21	3.89	3.43	2.87	2.51	7.89	3.21	2.44	3.46	3.46	1.56
	Knee	4.27	5.13	5.93	3.26	3.57	3.68	10.60	6.37	4.16	5.84	5.28	2.05
	Hip	11.06	5.78	4.05	12.24	3.19	6.15	3.43	3.69	2.22	3.71	5.55	3.25
Subject Average Max Error	Ankle	9.49	8.07	12.37	10.78	7.74	11.25	16.04	9.49	7.31	7.91	10.04	2.55
	Knee	14.19	12.19	19.04	9.77	9.32	11.30	23.40	14.67	12.74	13.66	14.03	4.08
	Hip	18.58	14.65	13.46	19.96	6.90	13.82	8.15	8.03	6.49	8.69	11.87	4.66
Individualized RMSE	Ankle	1.84	2.13	3.04	1.52	1.73	1.56	4.07	2.75	2.29	2.16	2.31*	0.75
	Knee	3.36	2.83	4.90	3.37	2.28	2.34	3.87	3.77	4.74	3.12	3.46*	0.85
	Hip	2.65	1.94	3.00	3.05	1.76	2.08	2.82	3.50	2.49	2.75	2.60*	0.52
Individualized Max Error	Ankle	4.95	4.09	11.58	2.67	5.08	3.68	7.05	4.20	7.40	4.75	5.55*	2.43
	Knee	6.49	4.46	19.54	6.27	6.59	2.92	8.77	6.53	13.75	7.50	8.28*	4.63
	Hip	8.26	3.77	17.89	6.09	4.95	1.84	6.95	10.17	4.47	4.24	6.86*	4.31

included in the training data to provide shape associated with kinematics changing with slope and speed. These changes are represented by the updated optimization problem statement:

$$\begin{aligned}
\underset{x}{\text{minimize}} \quad & \rho + \delta||\text{vec}(\frac{\partial^3}{\partial\varphi^3} + \Lambda_{ij}x)||_2 + \gamma||R||_2, \\
\text{such that} \quad & -\rho \leq \bar{\mathbf{d}}_{\varphi_i\chi_h} - \Lambda_{ih}x \leq \rho, \\
& R = \text{vec}(\bar{\mathbf{d}}_{\varphi_i\chi_l} - \Lambda_{il}x), \\
& R_{\min} < \underset{m}{\min}\,\Lambda_{im}x, \\
& R_{\max} > \underset{m}{\max}\,\Lambda_{im}x, \\
& \forall\ i = 1, 2, ..., 150, \forall\ m = 1, 2, \ldots, 100, \\
& \text{and } \forall h \in H, \forall l \in L,\ \forall j \in H \cap L, \qquad (4)
\end{aligned}$$

where H and L are the sets of high and low priority trajectories, respectively. The high priority trajectories are treated identically to all of the trajectories in (3). The difference between the low priority trajectories and the model, called R, is minimized using the L^2 norm. All other terms are identical to (3).

The optimization protocol shown in (4) seeks to minimize the residuals associated with the new high/low priority training distinction. Pareto optimization was performed to adjust the weight that each set of residuals had on the optimization, so that the distinction is enforced. The jerk coefficient was set to $\gamma =$ 1e-5 for both modeling problems and the coefficient $\delta = 0.05$ was used for the updated protocol (4).

E. Statistics

Throughout this paper we will discuss error using the root mean squared error (RMSE). This metric calculates the deviation of the designed trajectory or surface from the subject's experimental kinematics. The formula is $RMSE_{\eta_p} = \sqrt{\sum_{i=1}^{I}\sum_{j=1}^{J}(\mathbf{d}_{\varphi_i\chi_j\eta_p} - \bar{\mathbf{d}}_{\varphi_i\chi_j})^2/N}$ for $I = 150$ points in phase and $J = 27$ tasks ($N = I \cdot J = 4050$).

When comparing the basis model trained from mean trajectories and the modified model trained on individualized trajectories, the RMSE and max error from each subject are computed for each joint. The population of those values for all subjects at one joint are then statistically compared with a one-tailed t-test, using an alpha of 0.05, to see if the evaluated parameter has been significantly reduced.

III. Results

In this section, we first examine how our method for individualizing the training data reduces the error from each subject's kinematics across tasks. These individualized trajectories are used to generate the individualized model according to the modified optimization protocol (4), which is then compared to the basis model trained on inter-subject mean kinematics using the optimization scheme in (3). The RMSE should be interpreted as goodness of fit to the experimental data across all tasks, and max error shows the magnitude of the largest deviation of the tested trajectory set or model from the experimental data. One-tailed t-tests were conducted on the populations of RMSE and max error values from all subjects at each joint to see if individualization statistically improved the fit compared to baseline.

A. Individualized Training Trajectories

Table I shows the RMSE and max error across all tasks for the inter-subject mean and individualized trajectories compared to the experimental kinematic trajectories for each subject. (The models trained on these trajectories will be evaluated in the next section.) Averaged across all subjects, individualization at the ankle decreased the RMSE by 1.15° and the max error by 4.50°. The improvements in fit generally occurred immediately before and after push-off and heel strike, and individualization often adjusted these regions to match the individual. The individualized trajectories have significantly smaller RMSE across all subjects (p = 0.03) as well as significantly smaller max error ($p \ll 0.01$).

Individualization at the knee decreased RMSE by 1.82° and max error by 5.75°. The RMSE and max error are both significantly decreased with p-values of 0.01 and 0.006, respectively. At the hip, individualization reduced the RMSE by 2.95° and the max error by 5.01°. The decrease in max error stems from fitting peak flexion and extension by scaling the amplitude of the trajectory. There is a significant decrease upon individualization for RMSE (p = 0.008) and max error (p = 0.01).

TABLE II: RMSE and max error of the basis and individualized models across all tasks for each subject and joint compared to experimental data. The top two sections pertain to the basis model and the bottom two refer to the individualized model. Significantly decreased values are marked with a '*' and all values are reported in degrees.

		AB01	AB02	AB03	AB04	AB05	AB06	AB07	AB08	AB09	AB10	Mean	SD
Basis RMSE	Ankle	3.21	2.41	4.25	3.56	3.36	3.05	8.42	3.46	3.44	3.44	3.86	1.58
	Knee	3.93	6.34	7.12	4.12	4.92	5.23	11.34	7.46	4.59	6.30	6.14	2.09
	Hip	11.70	6.09	4.25	11.88	3.33	6.09	4.13	4.90	2.82	4.24	5.94	3.08
Basis Max Error	Ankle	12.49	8.05	11.76	7.88	10.49	6.93	19.76	14.13	9.04	8.35	10.89	3.88
	Knee	13.08	11.76	14.94	11.95	10.99	14.50	23.81	18.33	10.16	14.34	14.34	4.10
	Hip	18.84	12.80	12.58	20.94	5.77	12.81	10.72	10.21	5.96	8.11	11.87	4.98
Individualized RMSE	Ankle	3.22	2.96	3.66	3.29	2.44	2.99	4.00	4.60	3.56	4.08	3.48	0.60
	Knee	4.17	4.03	5.70	3.96	2.68	3.22	4.65	3.47	5.63	3.87	4.14*	0.92
	Hip	2.12	2.03	3.29	1.97	2.07	1.71	4.57	2.56	2.82	2.13	2.53*	.81
Individualized Max Error	Ankle	5.50	7.39	10.93	5.31	5.70	8.42	11.03	17.52	7.13	8.51	8.81	3.49
	Knee	13.69	9.43	10.41	14.44	9.52	12.12	12.06	16.37	15.36	19.45	12.28	2.45
	Hip	6.70	8.54	11.68	8.35	7.19	8.60	9.91	10.61	12.04	10.60	9.42	1.73

B. Individualized Model Error

Similar to the way that we analyzed the training trajectories, we compare the basis model (trained on mean trajectories) to the individualized model (trained on individualized trajectories) in terms of how well they fit a subject's experimental data. The models are analyzed by sampling the vector of the model surface that lies on the task in question and calculating the RMSE and max error when compared to the subject's experimental data at that task. The results of these calculations are reported in Table II.

Averaging across subjects, individualization of the ankle model decreased the RMSE by 2.68°, which roughly halves the error across all tasks. The max error decreased 2.08°. The ankle tends to have lower RMSE and max error than the other joints because of its smaller range of motion, but its relative RMSE improvement by 31% is the best of all joints. No statistically significant decrease was found between the basis and individualized model for RMSE or max error.

Individualization of the knee model decreased the RMSE by 1.55° on average. This result is better than the improvement seen in the training data, exemplifying the strengths of this predictive modeling technique. The max error also decreased on average 2.06°, with a decrease of 11.75° for Subject 7. Unlike the ankle, RMSE was significantly smaller ($p = 0.01$) but there was no significant decrease in max error.

The individualized hip model reduced the RMSE 1.18° and the max error 2.45°, which is the best of all joints. Notably, individualization caused a 12.59° decrease in max error for Subject 4 and a 12.14° decrease for Subject 1, showing that this individualization technique has the promise to greatly improve fit across multiple tasks. Similar to the other joints, the RMSE of the individualized hip model is significantly smaller than the basis model ($p = 0.002$), but no significant difference was observed in max error.

IV. Discussion

This individualization technique is a simple yet effective way to predict an individual's joint kinematics across all tasks based on a single personalized task. The method can easily be adapted to tune a prosthetic leg, changing the motion of the leg to match and enhance a patient's gait. In this study, the method of propagating individuality reduces the max error up to 86% at the trajectory level and up to 64% at the model level, while decreasing RMSE across all joints. Fig. 2 shows the joint kinematics and demonstrates how the modeling process reduced error for Subject 6. This subject was chosen for discussion because of their representative improvements at the ankle, knee, and hip.

A. Ankle Fit: Trajectory and Model

Models of ankle position must fit peak flexion before push-off and peak extension immediately following it. For Subject 6, individualizing the training trajectories from mean kinematics decreased the RMSE by 0.95° across all tasks. This subject presents with a larger range of motion than the inter-subject average and that directly affects the fit. When the model is trained for this individual, we see a modest improvement in fit of 0.06° RMSE. The individualized ankle residuals, seen in Fig. 2 (Ankle), show that the model tightly fits the level-ground task because the individual component is derived from this high-priority task as discussed in Section II-D. The greatest improvement in the individualized model is seen throughout the stance phase, where the model fits the subject's high-priority trajectory (black) with residuals close to zero. The large residual trend found in the basis model during push-off ($\varphi \approx 0.6$) is dramatically minimized after individualization, further reinforcing that the individual contribution found in the level-ground task is a good estimation of individuality at other tasks. Peak push-off flexion and extension, features that generally show the greatest individuality, are better fit by the individualized model with a max deviation of 4.97° for the -10° slope trajectory. The fit of the model tends to deteriorate as the slope of the terrain increases–these tasks tend to have the largest residuals across all subjects. As seen in Fig. 2 (Ankle), the individualization process removes much of the variability associated with this subject's individual contribution by centering the residuals around zero, effectively showing why the RMSE decreases.

B. Knee Fit: Trajectory and Model

Similar to the ankle, individualization at the knee shows good improvements at the trajectory level. At the knee, the most individuality is shown during terminal stance and

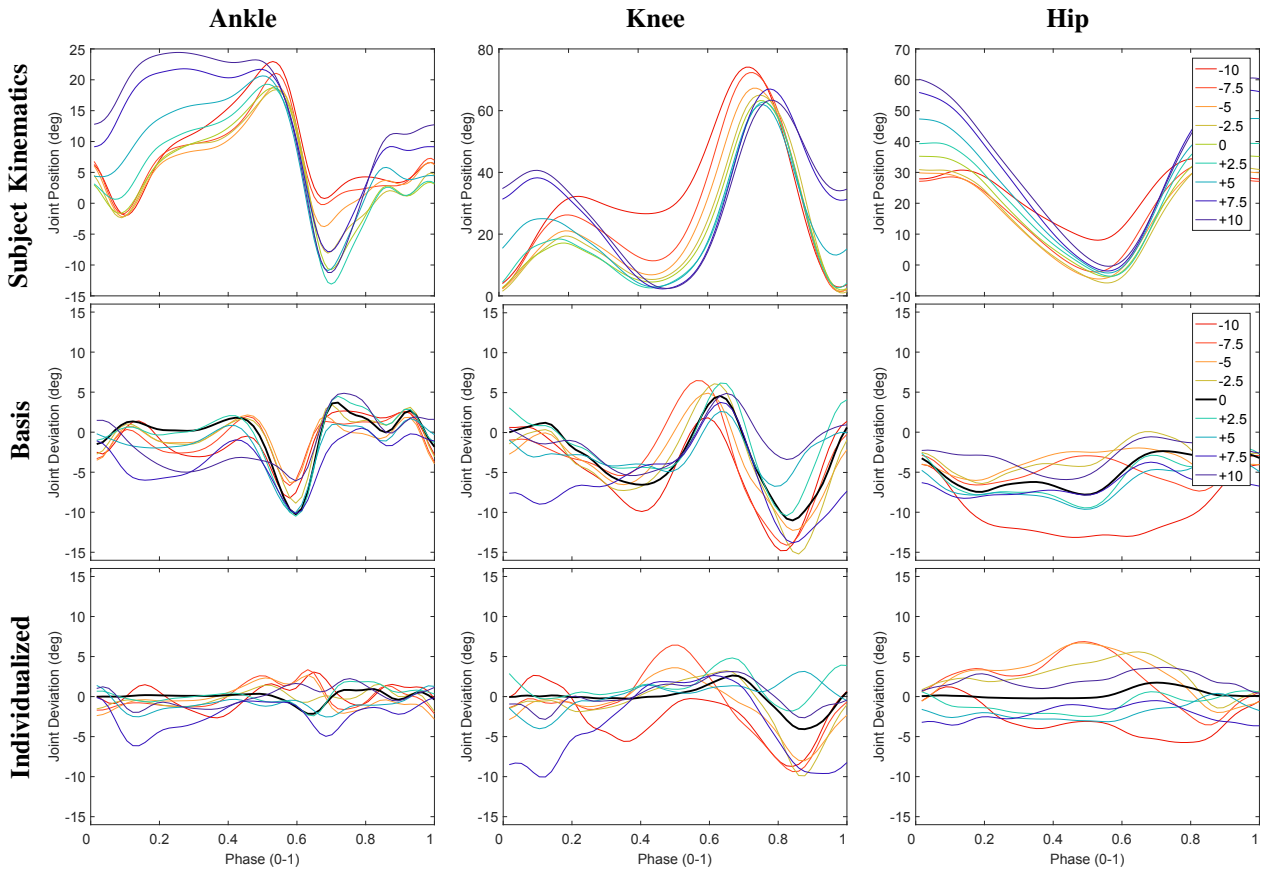

Fig. 2: Differences between the optimized models and Subject 6's experimental trajectories for normal speed at all inclines. Left to right show the ankle, knee, and hip joints. The top row shows the Subject 6's joint kinematics, the middle row shows the differences from the basis model and the bottom row shows the differences from the individualized model. The high-priority level-ground task is in bold black in the bottom two rows to emphasize how this trajectory is closely fit by the individualized model. The legend reports the inclines in degrees.

into the beginning of swing (Fig. 1). Our individualization method reduces the RMSE of the training trajectories by 1.34° compared to the mean trajectories. Individualization decreases the max error 63%, from 11.30° to 2.92°. This difference stems from the subject progressing through knee extension and flexion at a different point in the gait cycle, causing large residuals from the mean trajectories (which can also be seen at the model level in Fig. 2 (Knee)). As seen at the ankle, the individualized knee model tightly fits the level-ground task (black), with the RMSE decreasing 2.01° compared to the basis model. Tightly fitting this task reduces much of the error found during the stance phase by following the trend of most tasks. Occasionally, individualization deceases the efficacy of fit if one task shows an opposite trend as seen in the +10° task in Fig. 2 (Knee). For this task, the error increases around $\varphi = 0.1$ from -8.97° to -10.04°. Despite the effect seen around that task, individualization reduces the error across the majority of tasks by effectively centering the error around zero, further demonstrating the idea that trends in individuality hold across tasks. Further into terminal stance and through swing, the majority of error is reduced (the maximum deviation at this phase decreases from -14.22° to -8.90°), but notable errors still exist when experimental trajectories exhibit peak flexion and extension out of phase with the level-ground task. Individualization at the knee does not fully encompass the deviations seen at other tasks, but it does a good job of distributing the contribution to every task and decreasing error.

C. Hip Fit: Trajectory and Model

The hip joint is unique because of its kinematic symmetry along the phase axis (i.e., sinusoidal trajectory) and the fact that individualization generally scales the amplitude of the model to fit the subject's range of motion. With respect to the training trajectories, Subject 6 showed a great improvement upon individualization, reducing RMSE by 4.08° (a 45% decrease) and max error by 11.98°. Fig. 2 (Hip) demonstrates that the basis model consistently overestimates extension and flexion causing negative residuals across all tasks. The individualization process rectifies this consistent offset through the addition of the individual's contribution, seen in Fig. 2 (Hip). After individualization, the model showed a decrease in RMSE of 4.38° and decrease in max error of 4.21°. Upon investigation, the bulk of the error is observed in peak extension when the leg is extended behind the body before push-off. Individualization at this point increases the

error for some tasks, but decreases the max deviation seen at the +10° task in Fig. 2 (Hip) from -12.14° to -5.74°. The deviations seen for all subjects have similar trends after individualization, namely centering the error around zero and effectively reducing maximum error.

D. Modeling Considerations

Across all subjects and joints, we saw a good improvement in RMSE upon individualization with only 3 of 30 cases (10 subjects, 3 joints) showing a poorer fit at the training trajectory level and 8 of 30 at the model level (5 at the ankle joint). Despite this, the cases that showed a poorer fit after model individualization never showed an increased RMSE larger than 1.15°, which is small in practice. Moreover, the individualized models that showed improvements have RMSE reductions of up to 9.58° compared to the basis models. Throughout all cases the individualization process works best during stance phase (straightening the level-ground deviation around zero in Fig. 2), but there is room for improvement in fitting the quicker motions of swing phase.

Additionally, it is important to note that a small trade-off was made in the model fitting accuracy to minimize jerk, guarantee an anatomical range of motion, and avoid overfitting the data. In particular, the basis model presented in [15] can more accurately predict untrained tasks than linear interpolation, and we expect that benefit to extend to our individualized model. Another benefit of the basis modeling approach is the existence of an analytical derivative to control the desired joint velocity in robotic prosthetic legs [15].

It should be stressed that these models are fit to able-bodied kinematics, whereas prosthetists in a clinical setting typically tune a prosthesis to match and therapeutically enhance the amputee's gait. This study corroborates the assumption of individuality across tasks for able-bodied people, allowing for clinical individualization to be implemented to correct compensations of the amputee subject and make their gait more normative and symmetrical across all tasks.

V. Conclusion

Though this study was conducted with able-bodied data, the ease and efficacy of the presented individualization method can drastically reduce the time of tuning multiple tasks for powered prostheses, while remaining accessible to clinicians. This motivates the future development of a user interface, based on [1], to test this technique with clinicians and amputee subjects. With an interface utilizing this modeling technique, the desired kinematic output of the leg can be quickly and intuitively tuned to suit an amputee subject across a variety of tasks. We posit that this method of individualization will help the wearer reduce compensations across all tasks. Our work is a strong indicator that the limited data collected at level ground is still a powerful tool for improving walking performance at all slopes and speeds. Future work will extend this modeling and individualization technique to other ambulation tasks, such as climbing stairs of different inclinations and sit-to-stand.

References

[1] D. Quintero, E. Reznick, D. J. Lambert, S. Rezazadeh, L. Gray, and R. D. Gregg, "Intuitive Clinician Control Interface for a Powered Knee-Ankle Prosthesis: A Case Study," *IEEE J. Transl. Eng. Health Med.*, vol. 6, 2018.

[2] E. S. Gardinier, B. M. Kelly, J. Wensman, and D. H. Gates, "A controlled clinical trial of a clinically-tuned powered ankle prosthesis in people with transtibial amputation." *Clin. Rehab.*, vol. 32, no. 3, 2018.

[3] A. M. Simon, K. A. Ingraham, N. P. Fey, S. B. Finucane, R. D. Lipschutz, A. J. Young, and L. J. Hargrove, "Configuring a Powered Knee and Ankle Prosthesis for Transfemoral Amputees within Five Specific Ambulation Modes," *PLoS ONE*, vol. 9, no. 6, 2014.

[4] P. F. Pasquina, A. J. Carvalho, I. Murphy, J. L. Johnson, T. M. Swanson, B. D. Hendershot, M. Corcoran, B. Ritland, M. E. Miller, and B. M. Isaacson, "Case Series of Wounded Warriors Receiving Initial Fit PowerKnee™ Prosthesis," *J Prosthet Orthot.*, vol. 29, no. 2, 2017.

[5] M. Schaarschmidt, S. W. Lipfert, C. Meier-Gratz, H.-C. Scholle, and A. Seyfarth, "Functional gait asymmetry of unilateral transfemoral amputees," *Hum. Mov. Sci.*, vol. 31, no. 4, 2012.

[6] K. A. Ingraham, N. P. Fey, A. M. Simon, and L. J. Hargrove, "Assessing the Relative Contributions of Active Ankle and Knee Assistance to the Walking Mechanics of Transfemoral Amputees Using a Powered Prosthesis," *PLOS ONE*, vol. 11, no. 1, 2016.

[7] T. Elery, S. Rezazadeh, C. Nesler, J. Doan, H. Zhu, and R. D. Gregg, "Design and Benchtop Validation of a Powered Knee-Ankle Prosthesis with High-Torque, Low-Impedance Actuators," in *Pros. IEEE ICRA*, 2018.

[8] B. E. Lawson, J. Mitchell, D. Truex, A. Shultz, E. Ledoux, and M. Goldfarb, "A robotic leg prosthesis: Design, control, and implementation," *IEEE Robot. and Autom. Mag.*, 2014.

[9] F. Horst, S. Lapuschkin, W. Samek, K.-R. Müller, and W. I. Schöllhorn, "Explaining the Unique Nature of Individual Gait Patterns with Deep Learning," *Sci. Rep.*, 2019.

[10] F. Horst, M. Mildner, and W. Schöllhorn, "One-year persistence of individual gait patterns identified in a follow-up study – A call for individualised diagnose and therapy," *Gait Posture*, vol. 58, 2017.

[11] M. J. Major and N. P. Fey, "Considering passive mechanical properties and patient user motor performance in lower limb prosthesis design optimization to enhance rehabilitation outcomes," *Phys. Ther. Rev.*, vol. 22, no. 4, 2017.

[12] E. Chehab, T. Andriacchi, and J. Favre, "Speed, age, sex, and body mass index provide a rigorous basis for comparing the kinematic and kinetic profiles of the lower extremity during walking," *J. Biomech.*, vol. 58, 2017.

[13] F. Moissenet, F. Leboeuf, and S. Armand, "Lower limb sagittal gait kinematics can be predicted based on walking speed, gender, age and BMI," *Sci. Rep.*, vol. 9, no. 1, 2019.

[14] F. J. Diedrich and W. H. Warren, "The dynamics of gait transitions: Effects of grade and load," *J. Mot. Behav.*, 1998.

[15] K. R. Embry, D. J. Villarreal, R. L. Macaluso, and R. D. Gregg, "Modeling the Kinematics of Human Locomotion over Continuously Varying Speeds and Inclines," *IEEE T. Neur. Sys. Rehab.*, vol. 26, no. 12, 2018.

[16] D. Quintero, D. J. Villarreal, D. J. Lambert, S. Kapp, and R. D. Gregg, "Continuous-Phase Control of a Powered Knee-Ankle Prosthesis: Amputee Experiments Across Speeds and Inclines," *IEEE T. Robot.*, vol. 34, no. 3, 2018.

[17] K. Embry, D. Villarreal, R. Macaluso, and R. Gregg, "The effect of walking incline and speed on human leg kinematics, kinetics, and EMG," *IEEE DataPort*, 2018.

[18] T. Lenzi, L. Hargrove, and J. Sensinger, "Speed-adaptation mechanism: Robotic prostheses can actively regulate joint torque," *IEEE Robot. Automa. Mag.*, vol. 21, no. 4, 2014.

[19] T. Flash and N. Hogan, "The coordination of arm movements: an experimentally confirmed mathematical model," *J. Neurosci.*, vol. 5, no. 7, 1985.

[20] M. Grant and S. Boyd, *Graph implementations for nonsmooth convex programs*, ser. Lecture Notes in Control and Information Sciences. Springer-Verlag Limited, 2008.

[21] S. Boyd and L. Vandenberghe, *Convex Optimization*. Cambridge University Press, 2004.